# Spatio-temporal Validation of Multi-Source Satellite Rainfall Products in the Upper Tekeze-Atbara Basin, Ethiopia

**Achenafi Teklay**

**Citation**: Achenafi Teklay (2022) Spatio-temporal Validation of Multi-Source Satellite Rainfall Products in the Upper Tekeze-Atbara Basin, Ethiopia, *International Journal of Environment and Pollution Research*, Vol.10, No.2 pp.50-76

**ABSTRACT:** *Precise and reliable rainfall data is crucial for regional water resource management. However, rainfall data in Ethiopia mainly characterized by sparse distribution and temporal inconsistency. Therefore, the spatial and temporal patterns of rainfall are poorly understood in the major basins. Recently, satellite rainfall products (SRPs) have been applied as an alternative source to obtain long-term rainfall data. This study evaluated the performance of three different SRPs, namely CHIRPS, PERSIANN_CDR, and TMPA3B42, with respect to observed data in the Upper Tekeze-Atbara River Basin using different statistical indices. The result showed that PERSIANN_CDR had very low PBIAS than other products. The PERSIANN_CDR had a slight overestimation tendency, while the CHIRPS and TMPA3B42 considerably overestimated observation rainfall. The PERSIANN_CDR performed well for kiremt, belg, and bega season, with the lowest RMSE value of 2.9, 1.4, and 0.8 mm/day, respectively. On the contrary, TMPA3B42 poorly performed for kiremt, belg, and bega seasons with the largest RMSE value of 3.1, 1.9, and 1.1 mm/day, respectively. The PERSIANN_CDR had the best skill to detect observation rainfall, while the CHIRPS had the worst detecting skill during all seasons. In kiremt seasons, the PERSIANN_CDR product showed a good estimation of the observed rainfall almost in all parts of the basin except for a slight overestimation in northwestern and underestimation in southwestern regions. Overall, the findings of this study demonstrated the PERSIANN_CDR product potentials and use for analyzing rainfall distribution and variability in Ethiopia's Upper Tekeze-Atbara River Basin.*

**KEYWORDS**: validation, satellite rainfall products, PERSIANN_CDR, CHIRPS, TMPA3B42, spatio-temporal, Tekeze-Atbara

## INTRODUCTION

Accurate and quality rainfall data is very crucial for regional and global operational and research in water resource management, hydrological applications, and agricultural water use (Yong et al., 2010; Sunil Kumar et al., 2015; Guo and Liu, 2016). Rainfall variability in terms of intensity, volume, and pattern significantly affected the hydrological cycle (Stillman et al., 2014). As a result, precision rainfall measurement is essential for studying the spatial and temporal patterns of rainfall at various scales and expanding our understanding of the impact of rainfall on agriculture and hydrology (Awulachew et al., 2007; Ayalew et al., 2012). Rain gauges have traditionally been the primary source of rainfall data, as they have proven to be the most precise and reliable method of measuring rainfall (Ayehu et al., 2018).

However, in developing countries, weather stations are rare, unevenly distributed, and temporally inconsistent (Katsanos et al., 2016; Fenta et al., 2018). These issues are common especially in complex topography (Rivera et al., 2018), like Ethiopia's highlands, where rainfall varies greatly over short distances (Haile et al., 2009; Rientjes et al., 2012). The assessment of rainfall spatial distribution in remote locations in Ethiopia remains challenging due to lack of gauging stations (Hirpa et al., 2010; Ayehu et al., 2018; Igbal et al., 2018; Belay et al., 2019). Furthermore, the spatial and temporal analysis mainly based on a single or a few point-based rain gauge measurements, which may not represent the entire area (Belay et al., 2019). To avert these challenges, satellite-based rainfall estimation can be used to analyze the spatial and temporal variability of rainfall (Ayehu et al., 2018; Fenta et al., 2018; Alemu and Bawoke, 2019).

Recently, satellite rainfall products (SRPs) provide synoptic data at finer temporal and spatial resolutions (Park et al., 2017). The long-term rainfall data generated from satellite products can be used for hydrological simulation (Talchabhadel et al., 2021). However, satellite rainfall estimations are subjected to a certain bias attributed with gaps in revisit times, weak correlation between remotely sensed signals and rainfall rate, atmospheric effects that modify the radiation field and retrieval algorithms, and satellite instrument sensors (Fenta et al., 2018; Alemu and Bawoke, 2019). Therefore, investigating the performance of SRPs in specific region will provide information to the scientific communities and algorithm developers (Belay et al., 2019). Furthermore, validation of SRPs is very crucial before applying it for hydrological simulations and rainfall variability analyses (Dinku et al., 2007; Jiang et al., 2012; Ayehu et al., 2018).

Many studies have been conducted to evaluate different SRPs performances for hydrological applications (Katsanos et al., 2016; Hobouchian et al., 2017; Lakew et al., 2017; Zambrano-Bigiarini et al., 2017; Iqbal and Athar, 2018; Lekula et al., 2018; Rivera et al., 2018; Alemu and Bawoke, 2019). Thiemig et al. (2012) compared six SRPs with data from rain gauges in four river basins located in Africa. They found that all SRPs had high performance over the tropical wet and dry zone compared to semiarid mountainous regions, but low accuracy in detecting heavy rainfall events over semiarid areas and the number of rainy days in the tropics. Hessel (2015) compared ten SRPs over the Nile basin and recommended CHIRPS products for rainfall estimations. Belay et al. (2019) investigation showed that the CHIRPS product highly performed compared to others. Besides, the performance of SRPs has been evaluated in different climatic zones including Nzoia Basin along with Lake Victoria (Li et al., 2009), Ethiopian highlands (Hirpa et al., 2010; Gebrechorkos et al., 2017), Northern Tanzania (Mashingia et al., 2014), and western Uganda (Diem et al., 2014).

However, few studies have been undertaken in the Upper Tekeze-Atbara River Basin (UTARB) (Seleshi and Zanke, 2004; Gebremichael et al., 2017). The previous studies overlook comprehensive validation of spatio-temporal rainfall variability for the entire basin. For example, Seleshi and Zanke (2004) analyzed the rainfall pattern over the upper portion of the UTARB using single rain gauge station. Their result demonstrated that the amount of rainfall remained constant for the past 40 years (1962–2002). Gebremichael et al. (2017) evaluated the performance of eight SRPs (TRMM, CHIRPS, RFEv2, ARC2, PERSIANN, GPCP, CMAP and CMORPH) in UTARB. They examined SRPs with different spatial resolutions (0.05° to 2.5°) under wet season. This is the major drawback of their study. Because, the performance of SRPs highly correlated with spatial resolution. Therefore, this study was designed to investigate the performance of different SRPs which have the same spatial resolution. The measurement accuracy of SRPs are continuously improving because of advancements in sensor technologies and estimation techniques (Zhang et al., 2016). Several high resolutions SRPs are now available at a quasi-global scale (Behrangi et al., 2011; Jiang et al., 2012). The three widely used precipitation datasets namely; Climate Hazards Group Infrared Rainfall with Stations (CHIRPS), Precipitation Estimation from Remotely Sensed Information Using Artificial Neural Networks-Climate Data Record (PERSIANN_CDR), and The Tropical Rainfall Measurement Mission (TRMM) Multi-satellite Precipitation Analysis (TMPA), were evaluated in this study.

The purpose of this study is to assess the performance of the three SRPs using statistical indicators over the UTARB. The accuracy of these products was evaluated by using 45 observed rainfalls at daily, monthly, and seasonal scales from 2007 to 2017. In addition, this study is the first to undertake spatio-temporal validation and evaluation of each SRP's rain-detection ability over the UTARB.

## MATERIALS AND METHODS

### Study Area Description

Ethiopia's northwestern highlands are home to this research region. It is located on the Tekeze-Atbara River Basin, one of the Nile River's principal tributaries, and has a total catchment area of 66,543 km$^2$ at the Wad El-Hilew outflow, which includes Ethiopia, Eritrea, and Sudan. It is situated at 36.1° E – 39.5° E longitude and 11.4° N– 14.5° N latitude (Figure 1). The basin is characterized by rugged topography with a significant variation of elevation. Based on topographic information from the Shuttle Radar Topographic Mission (SRTM) Digital Elevation Model (DEM) the elevation ranges from 471 m above sea level (m.a.s.l) at North-western part to 4540 m.a.s.l at Ras Dejen Mountain.

The climate is the semi-arid climate within the east and north part of the basin, and partly semi-humid within the south with a high seasonal rainfall regime with strong interannual variation (Conway, 2000; Tamene et al., 2006; Belete, 2007). The 85 percent of the entire annual rainfall falls within the wet (Kiremt) season (June to September) which varies from 400 mm/yr within the Northeast at Humera to quite 1200 mm/yr within the Southwest near Ras Dejen Mountain (Figure

2). The variations are mainly related to the seasonal migration of the inter-tropical convergence zone (ITCZ). The annual start and finish of the ITCZ over Ethiopia's highlands fluctuate, causing inter-annual rainfall variability (Seleshi and Zanke, 2004; Nyssen et al., 2005). Rainfall is both a monomodal type (west of the basin) and a bimodal type within the east (quasi double maximum) rainfall pattern, with a little peak in May and a maximum peak in August (Figure 2).

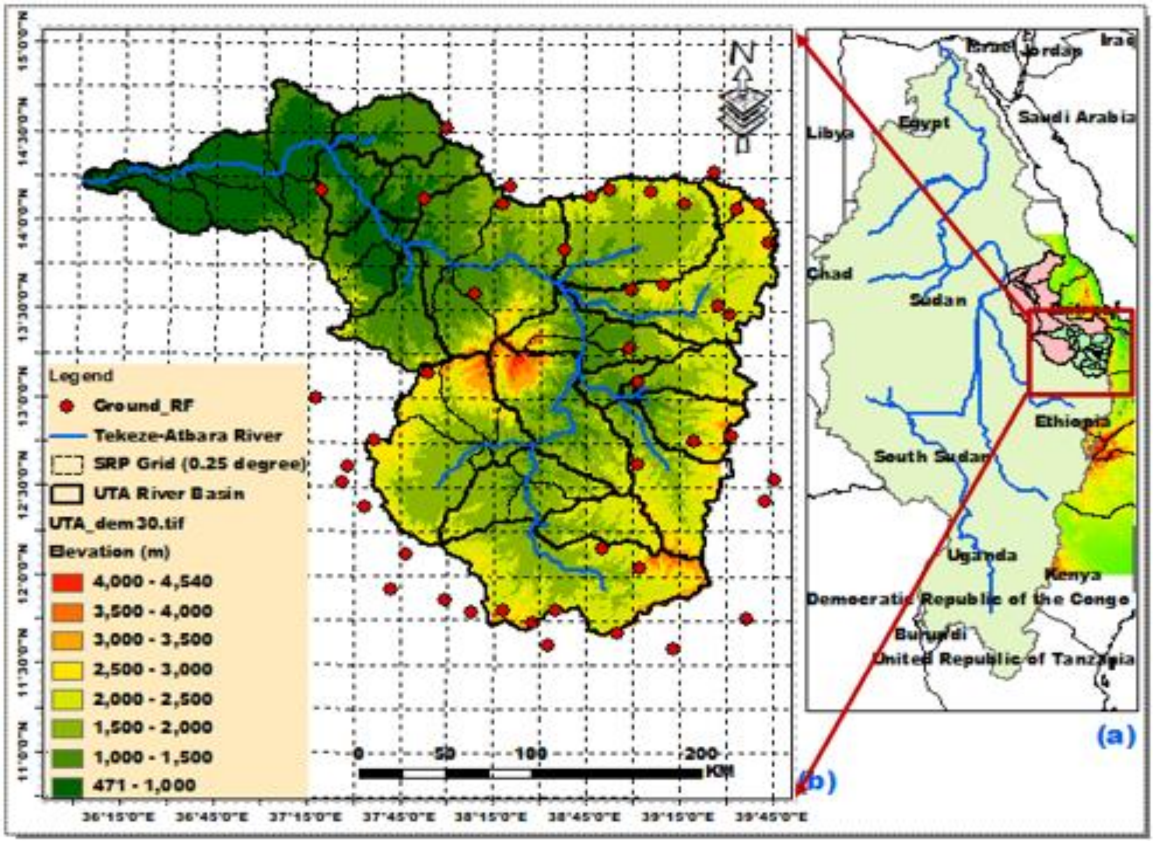


Figure 1. (a) Location of Blue Nile Basin, and (b) Upper Tekeze-Atbara River Basin with drainage pattern, observed rainfall, and topography map.

In Ethiopia, there are three distinct seasons (Bega, Belg, and Kiremt), each with differing rainfall amounts. The Bega is the dry season and is approximately defined by October through the end of February. Belg, approximately defined by March to the end of May, is considered the minor rainy season. The major rainy season, roughly defined as June to the end of September, is known as Kiremt. The major mechanism for rainfall during the Kiremt is the seasonal oscillation of the ITCZ (Seleshi and Zanke, 2004; Segele et al., 2008).

Although a great variation in elevation (471 to 4540 m.a.s.l) exists, much of the highland plateau is comprised between 1500 and 3000 m.a.s.l. The topography is mainly hilly, with notable, deeply incised valleys and volcanic rocky summits interspersed (Sutcliffe and Parks, 1999). The topographic roughness of the Upper Tekeze-Atbara River Basin is slightly higher, possibly due to the fragmentation of the plateau surface by numerous ephemeral rivers and erosion gullies (Tamene et al., 2006).

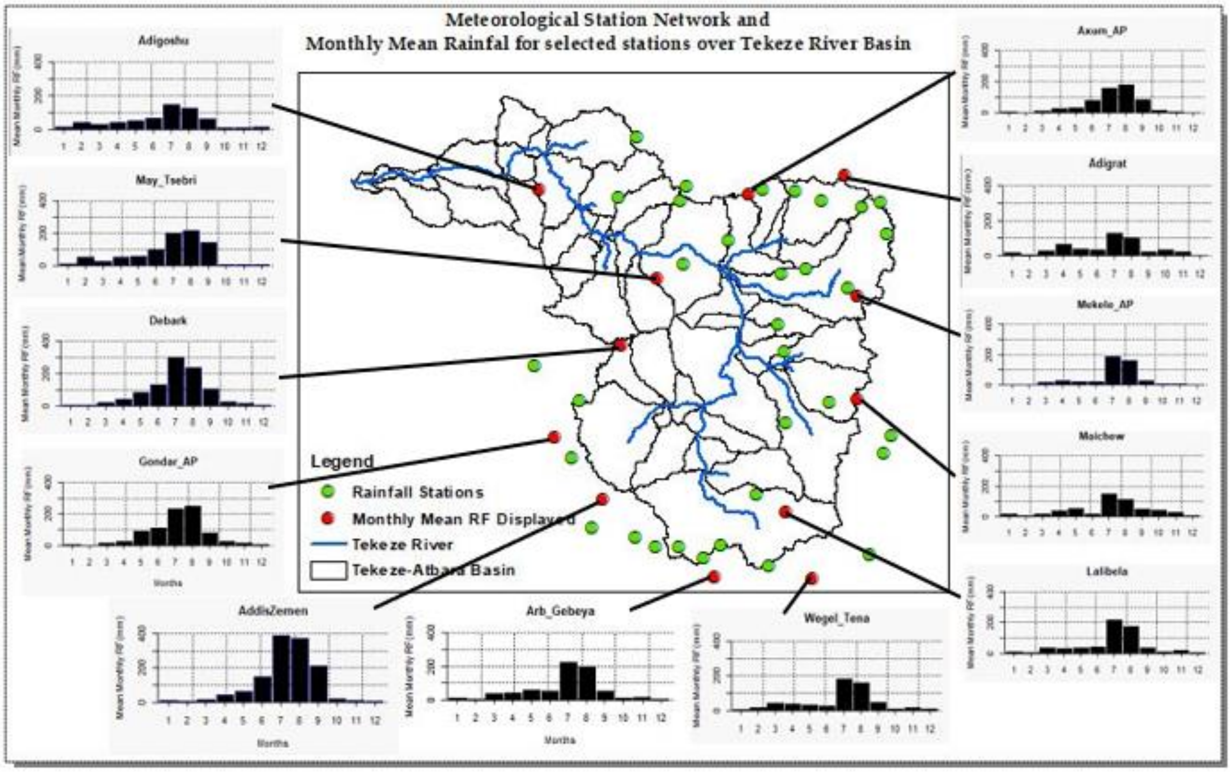


Figure 2. Rain gauge networks and monthly mean rainfall for selected stations over Upper Tekeze-Atbara River Basin for the period 2007-2017.

## Data Collection

### Observed Rainfall Data

Daily observed rainfall data within and around Upper Tekeze-Atbara River Basin were obtained from the National Meteorology Agency of Ethiopia (http://www.ethiomet.gov.et). The performance of satellite rainfall products was evaluated using 45 meteorological stations from 2007 to 2017 (Table 1).

Table 1. List of observed rainfall stations used for this study over the study area.

| Id | Name | Lat. | Long. | Elev. | Id | Name | Lat. | Long. | Elev. |
|---|---|---|---|---|---|---|---|---|---|
| 1 | Abi_Adi | 13.61 | 39.00 | 1829 | 24 | Gashena | 11.68 | 38.92 | 2969 |
| 2 | AddisZemen | 12.12 | 37.77 | 1940 | 25 | Gassay | 11.80 | 38.13 | 2789 |
| 3 | Adiawala | 14.52 | 37.99 | 1570 | 26 | Gondar AP | 12.52 | 37.43 | 1973 |
| 4 | Adigoshu | 14.17 | 37.31 | 1114 | 27 | HagereSelam | 13.65 | 39.17 | 2618 |
| 5 | Adigrat | 14.28 | 39.45 | 2497 | 28 | Lalibela | 12.04 | 39.04 | 2487 |
| 6 | Adwa | 14.18 | 38.88 | 1911 | 29 | Maichew | 12.78 | 39.53 | 2432 |
| 7 | Ager_genet | 11.80 | 38.30 | 3010 | 30 | Maksegnit | 12.39 | 37.55 | 1912 |

| | | | | | | | | | |
|---|---|---|---|---|---|---|---|---|---|
| 8 | Alamata | 12.42 | 39.71 | 1589 | 31 | MayTsebri | 13.59 | 38.14 | 1349 |
| 9 | Ambagiorgis | 12.77 | 37.60 | 2900 | 32 | MekeleAP | 13.47 | 39.53 | 2257 |
| 10 | Arb_Gebeya | 11.60 | 38.54 | 2567 | 33 | MekeleOB | 13.52 | 39.47 | 2000 |
| 11 | Atsebi | 13.88 | 39.74 | 2711 | 34 | Nebelet | 14.10 | 39.28 | 1988 |
| 12 | Axum_AP | 14.14 | 38.78 | 2113 | 35 | Nefasmewucha | 11.73 | 38.47 | 3098 |
| 13 | Aynbugna | 12.15 | 38.83 | 2000 | 36 | Sanja | 12.99 | 37.29 | 1003 |
| 14 | Chercher | 12.54 | 39.77 | 1781 | 37 | Sekota | 12.63 | 39.03 | 2258 |
| 15 | Debark | 13.14 | 37.90 | 2836 | 38 | Semema | 14.19 | 38.34 | 1948 |
| 16 | DebreZebit | 11.81 | 38.58 | 3220 | 39 | Senkata | 14.06 | 39.57 | 2437 |
| 17 | DebreTabor | 11.87 | 37.99 | 2612 | 40 | Shire | 14.10 | 38.29 | 1897 |
| 18 | EdagaSelus | 13.84 | 38.63 | 2057 | 41 | Sirinka | 11.75 | 39.61 | 1861 |
| 19 | Edagarbu | 14.09 | 39.69 | 2920 | 42 | Wedisemro | 12.76 | 39.34 | 2456 |
| 20 | Mayyohannes | 14.12 | 37.87 | 1116 | 43 | Wegel_Tena | 11.59 | 39.22 | 2951 |
| 21 | Feresmay | 14.17 | 39.10 | 1948 | 44 | Woreta | 11.92 | 37.70 | 1819 |
| 22 | Finarawa | 13.10 | 39.02 | 1500 | 45 | Yechila | 13.28 | 38.98 | 1591 |
| 23 | Dimma | 13.68 | 38.32 | 1626 | | | | | |

**Satellite Rainfall Products (SRPs)**

In this study, the performance of three high-resolution SRPs, namely the Tropical Rainfall Measuring Mission (TRMM) Multi-satellite Precipitation Analysis (TMPA) 3B42 version 7 algorithm (hereafter TMPA 3B42), the Climate Hazards Group Infrared Precipitation Stations (CHIRPS), and the Precipitation Estimation from Remotely-Sensed Information using Artificial Neural Networks - Climate Data Record (PERSIANN_CDR), were evaluated.

**TMPA 3B42 Rainfall Data**

The TMPA3B42 version 7 is a gauge-adjusted product and launched by the National Aeronautics and Space Administration NASA and the Japanese Aerospace Exploration Agency (JAXA) to monitor precipitation in the tropical and subtropical areas of 50° S – 50° N (Huffman and Bolvin, 2010). This product has 0.25° × 0.25° spatial resolution and is available from 1998 to 2015 in the 3-hours interval. Daily TRMM 3B42 v7 (TMPA 3B42) data is obtained by summing the 3-hourly precipitation. The daily rainfall data for the period 2007–2017 were obtained from the TRMM webpage (https://disc.gsfc.nasa.gov). More information about the TRMM products is given by Huffman and Bolvin (2010).

**CHIRPS Rainfall Data**

The CHIRPS version 2 is a quasi-global (50º S - 50º N), and daily gridded product with a spatial resolution of 0.05º and 0.25º (Funk et al., 2015). It is designed for monitoring agricultural drought and global environmental change over land, and it also can be used to force hydrologic models and simulate near-real-time initial hydrologic conditions (Funk et al., 2015). CHIRPS is a third-generation rainfall technique that uses a variety of interpolation schemes to generate spatially continuous grids from raw point data (Husak et al., 2007). The "satellite-gauge" category includes the CHIRPS rainfall product (Table 2).  Daily CHIRPS products at the spatial resolution of 0.25°

are available from 1981 to the present. In this study, the data for the period 2007-2017 were downloaded (ftp://chg-ftpout.geog.ucsb.edu/pub/org/chg/products/CHIRPS-2.0). Funk et al. (2015) provide more extensive information about CHIRPS.

Table 2. Summary of the satellite rainfall products used in this study.

| SN | Rainfall Products | Data Input | Spatial resolution | Temporal resolution | Data Source |
|---|---|---|---|---|---|
| 1 | TMPA 3B42V7* | PMW + IR + satellite radar + gauge | 0.25° | Daily | O, & S |
| 2 | PERSIANN_CDR V1R1* | PMW (GPCP v2.2) + IR + gauge + ANN | 0.25° | Daily | O, & S |
| 3 | CHIRPSV2.0** | IR + TMPA3B42+gauge + CHPclim | 0.25° | Daily | O, S, & R |

Note: * Multi-satellite, **Infrared Estimate; O = Observed; S = Satellite; and R = Reanalysis.

**PERSIANN_CDR Rainfall Data**

The PERSIANN algorithm uses an artificial neural network (ANN) model to estimate precipitation using IR. Adaptive network parameter change utilizing rainfall estimations from a passive microwave sensor improves the accuracy of PERSIANN. A new product dubbed the PERSIANN CDR (for Climate Data Record) was generated by applying the PERSIANN algorithm to Gridded Satellite Infrared Data (GridSat-B1) and then bias correcting estimates using monthly precipitation data (Ashouri et al., 2015). The daily PERSIANN_CDR product has been available for near-global coverage (60° S–60° N) with a spatial resolution of 0.25° since 1983. The data for the period 2007-2017 were retrieved from the Center for Hydrometeorology and Remote Sensing (CHRS), University of California Irvine (http://chrsdata.eng.uci.edu). A detailed description of the PERSIANN_CDR algorithm is found in Ashouri et al. (2015).

**Performance Evaluation**

The performance of SRPs was evaluated through different statistical measures including categorical, continuous, and spatial comparison methods.

**Categorical Validation Statistics**

The rainfall detection capabilities of the SRPs were evaluated using a contingency table (Table 3). Four different combinations of estimated and observed data were used to test the frequency of correct and wrong estimated values. These combinations are: a Hit (H) when rainfall is recorded by both satellite and rain gauge; a Miss (M) when rain is only observed by the rain gauge; a False Alarm (F) when rain is only documented by satellite; and a Null when no rain is recorded by both satellite and rain gauge.

Table 3. Contingency table between observed rainfall and SRPs estimation.

| | | Observed rainfall | | |
|---|---|---|---|---|
| | | Rain | No-rain | Total |
| Satellite Rainfall Products (SRPs) | Rain | Hit (H) | False Alarm (F) | H + F |
| | No-rain | Miss (M) | Null (n) | M + n |
| | Total | H + M | F + n | Total rainfall events |

To evaluate the rain-detection capabilities of SRPs, categorical statistical indicators such as the probability of detection (POD), false alarm ratio (FAR), critical success index (CSI), and volumetric indices were utilized. POD is a measure of rain events that were successfully detected by the satellite (Equation 1), FAR is a measure of rain events that were mistakenly detected (Equation 2), and CSI is a measure of relative accuracy (Equation 3). The best POD and CSI values are 1, while the best FAR value is 0 (Khan et al., 2011; Moazami et al., 2013).

$$POD = \frac{H}{H + M} \tag{1}$$

$$FAR = \frac{F}{H + F} \tag{2}$$

$$CSI = \frac{H}{H + M + F} \tag{3}$$

Moreover, the volumetric indices that include Volumetric Miss Ratio (MRV) and Volumetric False Ratio (FRV) were used to evaluate the volumetric performance of the selected SRPs. The ratios value of MRV (Equation 4) to FRV (Equation 5) close to one indicate a balanced missed and false detection rain volumes. To define whether there is a rain or no rain event, a threshold value $\geq$1.0 mm/day was adopted (Gao and Liu, 2013; Moazami et al., 2013).

$$MRV = \frac{\sum(O|O = 0 \,\&\, S > 0)}{\sum(O)} \tag{4}$$

$$FRV = \frac{\sum(S|O = 0 \,\&\, S > 0)}{\sum(O)} \tag{5}$$

Where H is the hit; M is the miss, F is a false alarm, O is the observed rainfall, and S is satellite rainfall estimation.

**Continuous Validation Statistics**

The common continuous statistics including coefficient correlation (CC), root mean square error (RMSE), percent of bias (PBIAS), and coefficient of determination ($R^2$) were used to evaluate SRPs performance in estimating the amount of rainfall. CC measures the degree of association between the observation and satellite estimations (Equation 6). Positive correlation implies that when one quantity increases, the other one increases and vice-versa. If it's negative, it implies that when one quantity increases, the other decreases and vice-versa. The RMSE is a measure of the error in terms of the difference between satellite estimation and observation (Equation 7). The lower RMSE values indicate the smaller the errors in satellite estimation. The PBIAS is used to measure the average difference between observation and satellite estimation (Equation 8). The

PBIAS ranges from -∞ to +∞, where the value of zero represents the best satellite estimation performance. A positive value of PBIAS indicates SRP overestimation bias, and a negative value of PBIAS indicates SRP underestimation bias. $R^2$ describes the fraction of the variance in observation data by the satellite estimation (Equation 9). It is the magnitude linear relationship between the observed and the satellite values. $R^2$ ranges from 0 which indicates poor model performance to 1 which indicates best model performance, and typical values greater than 0.6 are considered acceptable model performance (Santhi et al., 2001).

$$CC = \frac{\sum(S - Sav)\,(O - Oav)}{\sqrt{\sum(S - Sav)^2}\,\sqrt{\sum(O - Oav)^2}} \quad (6)$$

$$RMSE = \sqrt{\frac{\sum(O - S)^2}{N}} \quad (7)$$

$$PBIAS = \frac{\sum(S - O)}{\sum(\,O\,)} * 100 \quad (8)$$

$$R^2 = \left(\frac{\sum(S - Sav)\,(O - Oav)}{\sqrt{\sum(S - Sav)^2}\,\sqrt{\sum(O - Oav)^2}}\right)^2 \quad (9)$$

Where: O = the observed rainfall, Oav= the observed mean rainfall, S = the satellite rainfall product estimation, Sav = the mean satellite rainfall product, and N = the number of rainfall events.
Besides, the cumulative distribution function (CDF) for the proportion of rainfall events, scatter plot, Taylor diagram, and graphs at daily, monthly, and seasonal time scales were used to evaluate rainfall estimation performance of the three SRPs.

### Spatial Comparisons

The spatial simulation performance of SRPs was assessed through a comparison of the observed and estimated rainfall map. The spatial rainfall maps were developed using the Kriging method. The advantage of Kriging is an estimation of an average value that takes account of the spatial correlation pattern of rainfall and quantification of an error (Boston et al., 2012). Only grid boxes with at least one gauge were used in the validation computation to avoid difficulties caused by the gauge network's sparseness (Diro et al., 2009).

## RESULTS

### Temporal Rainfall Estimation

#### Daily Rainfall

The daily comparison between SRPs and observed rainfall is shown in Table 4. All the SRPs overestimated the observed rainfall. The three SRPs had a very good correlation with observed rainfall, with CC values between 0.80 and 0.82. The lowest and highest association were found in PERSIANN_CDR and TMPA 3B42 products, respectively. The lowest RMSE value (1.94 mm/day) was found from the PERSIANN_CDR product, while the highest RMSE (2.72 mm/day) was recorded in the CHIRPS product. The PERSIANN_CDR product slightly overestimated the

Print ISSN: 2056-7537(print),
Online ISSN: 2056-7545(online)

observed rainfall, with a PBIAS value of 5.3% (Table 4). However, the CHIRPS and TMPA 3B42 product considerably overestimated the observed rainfall by 23.0% and 18.8%, respectively. Overall, the PERSIANN_CDR product captured very well the observed daily rainfall compared to TMPA 3B42 and CHIRPS.

Table 4. Summary of statistical comparison between daily observation rainfall and SRPs estimation over the UTARB for the period 2007-2017. Note: the observed daily mean rainfall is 1.93 mm/day.

| Satellite rainfall products | Mean (mm/day) | CC | RMSE (mm/day) | PBIAS |
|---|---|---|---|---|
| PERSIANN_CDR | 2.03 | 0.82 | 1.94 | 5.3 |
| CHIRPS | 2.37 | 0.81 | 2.72 | 23.0 |
| TMPA 3B42 | 2.29 | 0.80 | 2.15 | 18.8 |

The scatter plot of the daily observed rainfall versus SRPs for the period 2007-2017 is shown in Figure 3. The PRSIANN_CDR product captured well the observed rainfall, whereas the performance of the TMPA 3B42 product was more limited. All three SRPs tended to overestimate the observed rainfall. The overestimation from the TMPA 3B42 product was more pronounced where the observed rainfall was maximal. Most of PRSIANN_CDR estimations were relatively low deviation from best fit values ($R^2$ = 0.68), while the TMPA 3B42 estimations were high deviation ($R^2$ = 0.64).

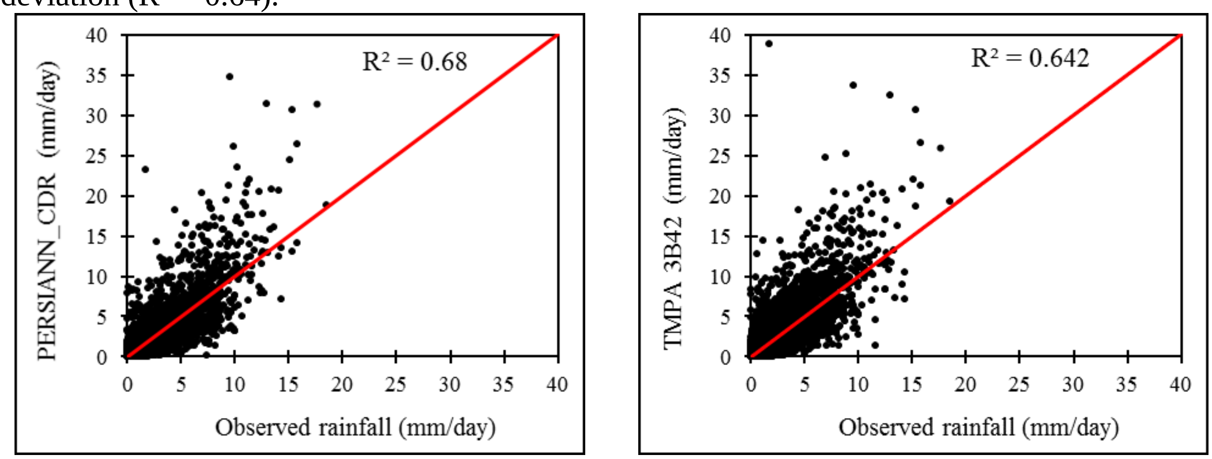

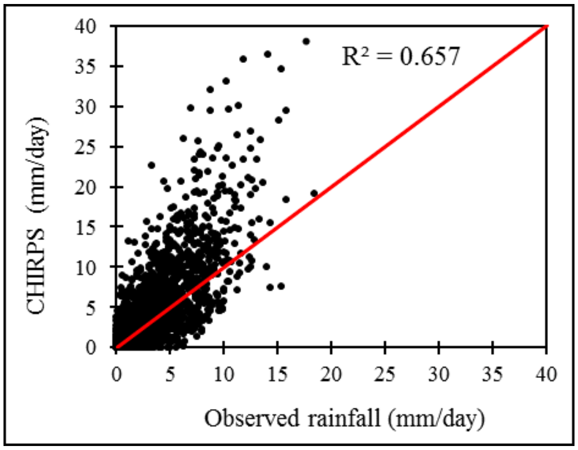


Figure 3. Scatter plot of daily rainfall: observations (x-axis) versus SRPs estimations (y-axis).

The Cumulative Distribution Function (CDF) of daily rainfall between the SRPs and observation is presented in Figure 4. Regarding daily rainfall values from 2007 to 2017, the observed highest rainfall was 18.47 mm/day (Figure 4a). However, the three SRPs estimated significantly higher than the observed maximum rainfall value. The highest daily rainfall from PERSIANN_CDR, TMPA 3B42, and CHIRPS products were 34.81, 38.51, and 38.07 mm/day, respectively. The estimated rainfall from PERSIAN_CDR and TMPA 3B42 product was slightly higher than the observed rainfall within the 10% frequency level. However, the CHIRPS rainfall estimations were extremely higher than the observation rainfall with this frequency. For example, the observed rainfall at a 5% frequency level was 7.7 mm (Figure 4a). At the same frequency level, PERSIAN_CDR and TMPA 3B42 estimations were 8.9 mm and 9.6 mm, respectively, while CHIRPS estimation was 11.3 mm. Moreover, the rainfall estimation from the PERSIANN_CDR product was very close to the observed rainfall in most frequency levels. As shown in Figure 4b, the number of rainfalls below 5 mm/day accounted for 12.75% and 13.3% of the observed and PERSIANN_CDR data, respectively. However, the number of rainfalls for this class was 16.3 % and 17.5% of CHIRPS and TMPA 3B42 data, respectively. This indicates that the PERSIANN_CDR estimation was close to the observed values in the daily time series.

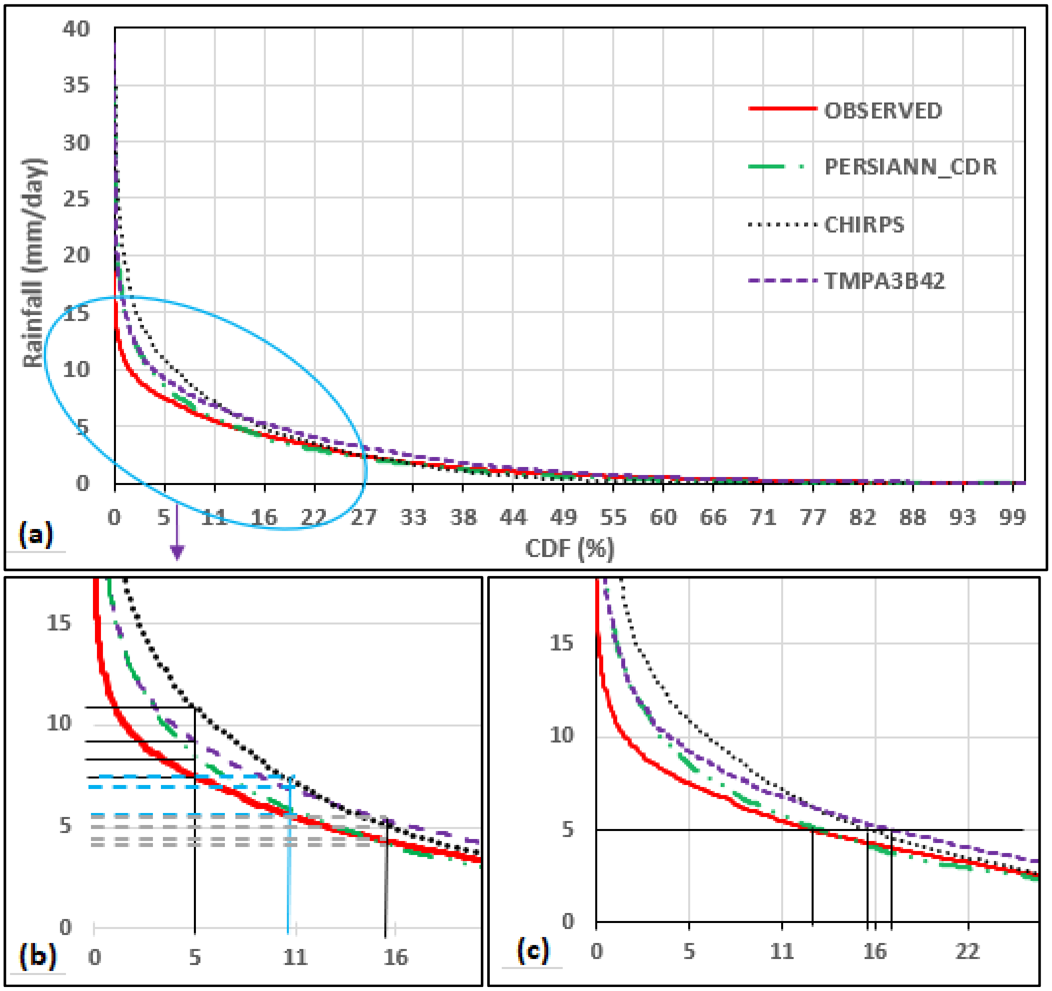


Figure 4. (a) Cumulative distribution function (CDF) of daily rainfall for rain gauge and the three SRPs over the UTARB for a period 2007-2017, b) rainfall at 5, 10, & 15% of frequency, and c) different frequencies at 5 mm of rainfall.

All the three SRP estimations had a strong agreement with the observed rainfall. The PERSIANN_CDR and TMPA 3B42 generally agreed well with the observed daily mean rainfall, with slightly lower RMSE and higher correlation (Figure 5a). The spatial variability in all SRPs estimation was higher than that of the observed rainfall (2.6 mm/day). The spatial variation in the CHIRPS product was considerably higher than the observed rainfall. In general, the PERSIANN_CDR product performed very well in estimating the observed rainfall, with the lowest RMSE (1.94 mm/day) and spatial variability (3.5 mm/day) and the highest correlation (0.83). On the contrary, the CHIRPS product performed poorly, with the highest RMSE (2.7 mm/day) and spatial variation (4.3 mm/day), and the lowest pattern correlation (0.8).

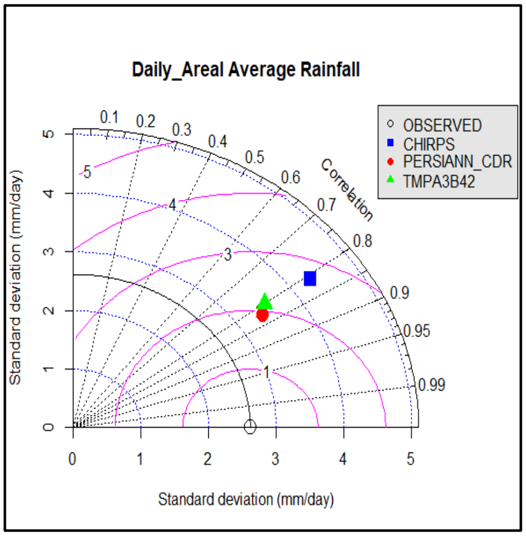


(a) (b)

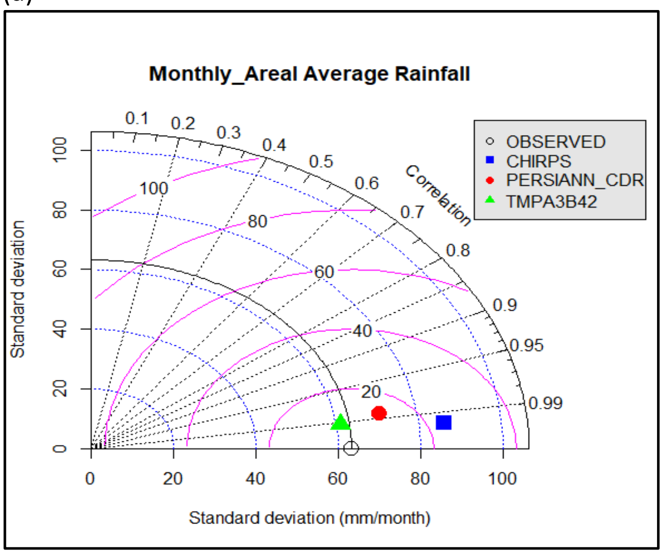


Figure 5. Taylor diagram showing a statistical comparison between SRPs and observed rainfall at; a) Daily, and b) Monthly areal average

**Monthly Rainfall**

The monthly rainfall analysis was carried out by summing daily rainfall for the period 2007–2017. All the three SRPs had a very strong association with the monthly observed rainfall (0.94-0.96) (Table 5), which shows significant improvement compared to daily time scales (0.80-0.82) (Table 4). The PERSIANN_CDR had the lowest RMSE (22.7 mm/month) and PBIAS (5.3%), while the CHIRPS had the highest RMSE (36.5 mm/month) and PBIAS (23%) (Table 5). General, the monthly estimation from the PERSIANN_CDR product reproduced the observed rainfall.

International Journal of Environment and Pollution Research
Vol.10, No.2 pp.50-76, 2022
Print ISSN: 2056-7537(print),
Online ISSN: 2056-7545(online)

Table 5. Summary of statistical comparison between monthly observation rainfall and SRPs estimation over the UTARB for the period 2007-2017. Note: the observed mean monthly rainfall is 56.65 mm/month.

| Satellite rainfall products | Mean (mm/month) | CC | RMSE (mm/month) | PBIAS |
|---|---|---|---|---|
| PERSIANN_CDR | 61.8 | 0.96 | 22.7 | 5.3 |
| CHIRPS | 72.1 | 0.95 | 36.5 | 23 |
| TMPA 3B42 | 69.7 | 0.94 | 28.6 | 18.8 |

Observed and SRPs estimated mean monthly rainfall for the period from 2007 to 2017 is shown in Figure 6. The CHIRPS estimated the largest and the smallest average monthly rainfall in August (264.6 mm/month) and December (4.2 mm/month), respectively. All the SRPs overestimated the observed rainfall in the wet months (July and August) and the dry months (October and November), while they underestimated the observed rainfall in February and March. The highest overestimation (68 mm/month) occurred in July in the CHIRPS product. Overall, the rainfall estimation from the PERSIANN_CDR product captured very well the observed rainfall in all months except May, June, and August (Figure 6).

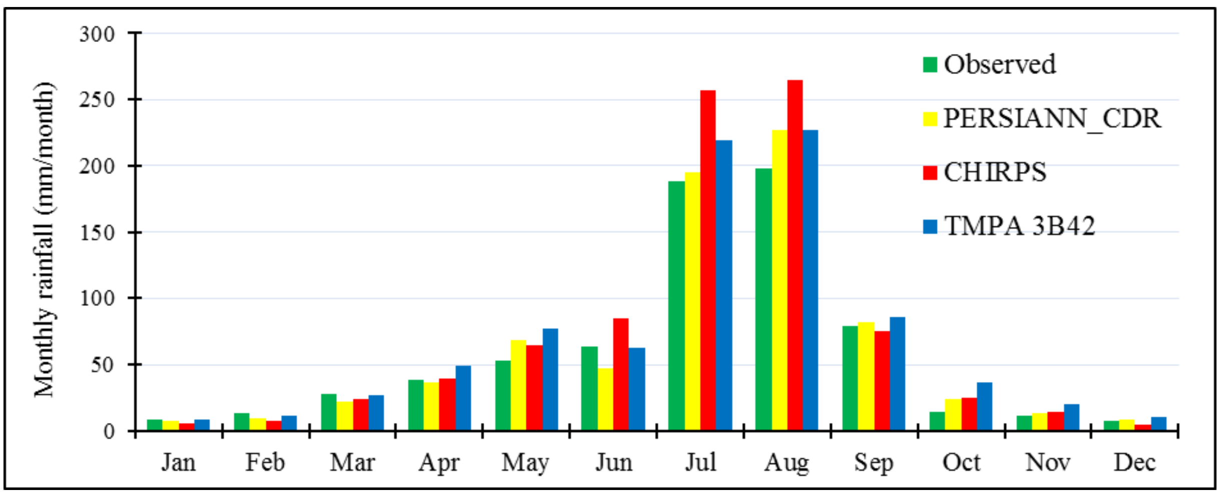

Figure 6. Long-term monthly areal mean rainfall (2007-2017) from observed and SRPs.

**Seasonal Rainfall**

Table 6 presents the comparison between observed and SRPs rainfall estimation on a seasonal basis. The correlation between observed and estimated rainfall in the PERSIANN_CDR and CHIRPS products was strong during the Belg season (Semi-dry season = February to May) (Table 6), the PERSIANN_CDR had the lowest RMSE (1.39 mm/day) and the TMPA 3B42 had the highest (1.86 mm/day). The PERSIANN_CDR and CHIRPS products slightly overestimated belg season rainfall. However, TMPA 3B42 significantly overestimated the observed belg season rainfall (24.7%). In kiremt season (Wet season = June to September), the three SRPs had a very good correlation with the observed rainfall, with the highest CC in PERSIANN_CDR (0.76). Besides, PERSIANN_CDR estimated the lowest RMSE value (2.94 mm/day) compared to other products. All three SRPs overestimated the observed rainfall during the kiremt season. The lowest overestimation was recorded from PERSIANN_CDR (4.2%), while the highest overestimation was found in CHIRPS (28.6%). In the bega season, the correlation between observed and estimated rainfall from the three products was poor (Table 6). The PERSIANN_CDR had the lowest error variance (0.8 mm/day), while TMPA 3B42 had the highest RMSE value (1.06 mm/day) in the bega season. The CHIRPS had the lowest PBIAS (17.9%) in the bega season, which indicates a slight overestimation of the observed rainfall. However, TMPA 3B42 significantly overestimated the observed rainfall, with a PBIAS value of 80.8%. Overall, the PERSIANN_CDR product represented well the observed rainfall in all three seasons.

Table 6. Summary of statistical comparison between seasonal observation rainfall and SRPs estimation over the UTARB for the period 2007-2017.

| Season | Statistical measures | Observed rainfall | Satellite Rainfall Products (SRPs) | | |
|---|---|---|---|---|---|
| | | | PERSIANN-CDR | CHIRPS | TMPA 3B42 |
| Belg | Mean | 1.10 | 1.14 | 1.12 | 1.38 |
| | CC | - | 0.69 | 0.68 | 0.60 |
| | RMSE | - | 1.39 | 1.70 | 1.86 |
| | PBIAS | - | 3.1 | 2.0 | 24.7 |
| Kiremt | Mean | 4.34 | 4.52 | 5.58 | 4.88 |
| | CC | - | 0.76 | 0.73 | 0.74 |
| | RMSE | - | 2.94 | 4.30 | 3.05 |
| | PBIAS | - | 4.2 | 28.6 | 12.5 |
| Bega | Mean | 0.34 | 0.43 | 0.40 | 0.61 |
| | CC | - | 0.63 | 0.59 | 0.59 |
| | RMSE | - | 0.80 | 0.90 | 1.06 |
| | PBIAS | - | 27.4 | 17.9 | 80.8 |

**Spatial Rainfall Estimation**

PERSIANN_CDR and CHIRPS demonstrated a good estimating tendency for observed rainfall in the northern half of the basin during the belg season (Figure 7). Both products, however, understated the amount of rain that fell on the northernmost reaches of the study area. The observed rainfall was well recreated by TMPA 3B42 in the northern and southern parts of the basin, while it was overestimated in the middle region.

Print ISSN: 2056-7537(print),
Online ISSN: 2056-7545(online)

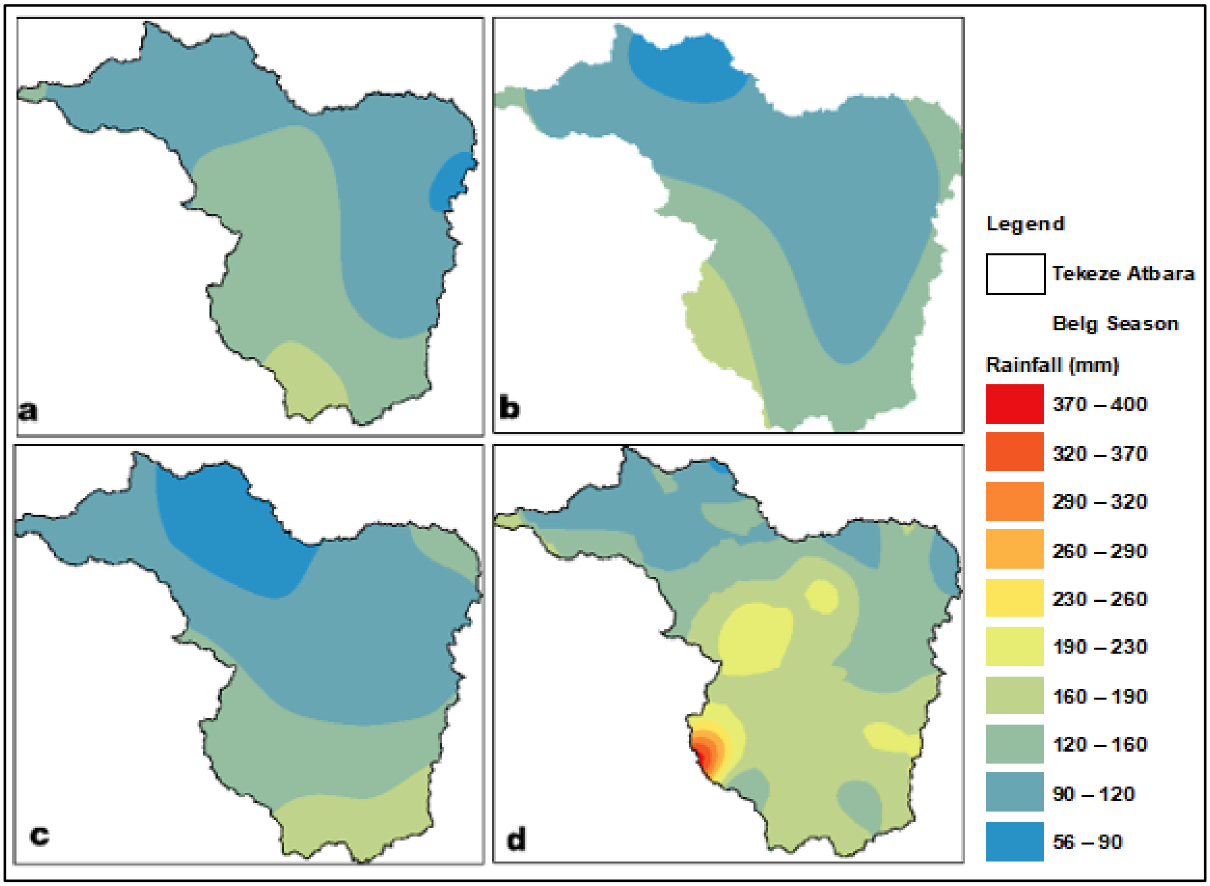


Figure 7. Comparison of the spatial pattern of mean season rainfall for the Belg season (February to May), a) Observed, b) PERSIANN_CDR, c) CHIRPS, and d) TMPA 3B42 over the UTARB for the period 2007-2017.

In kiremt seasons, the PERSIANN_CDR product showed a good estimating of the observed rainfall almost in all parts of the basin except for a slight overestimation in northwestern and underestimation in southwestern regions (Figure 8). CHIRPS product considerably overestimated rainfall in the northern part of the basin. TMPA 3B42 product estimated well the observed rainfall in the central and northeastern, while it showed overestimation and underestimation tendency in the northwestern and southwestern part, respectively.

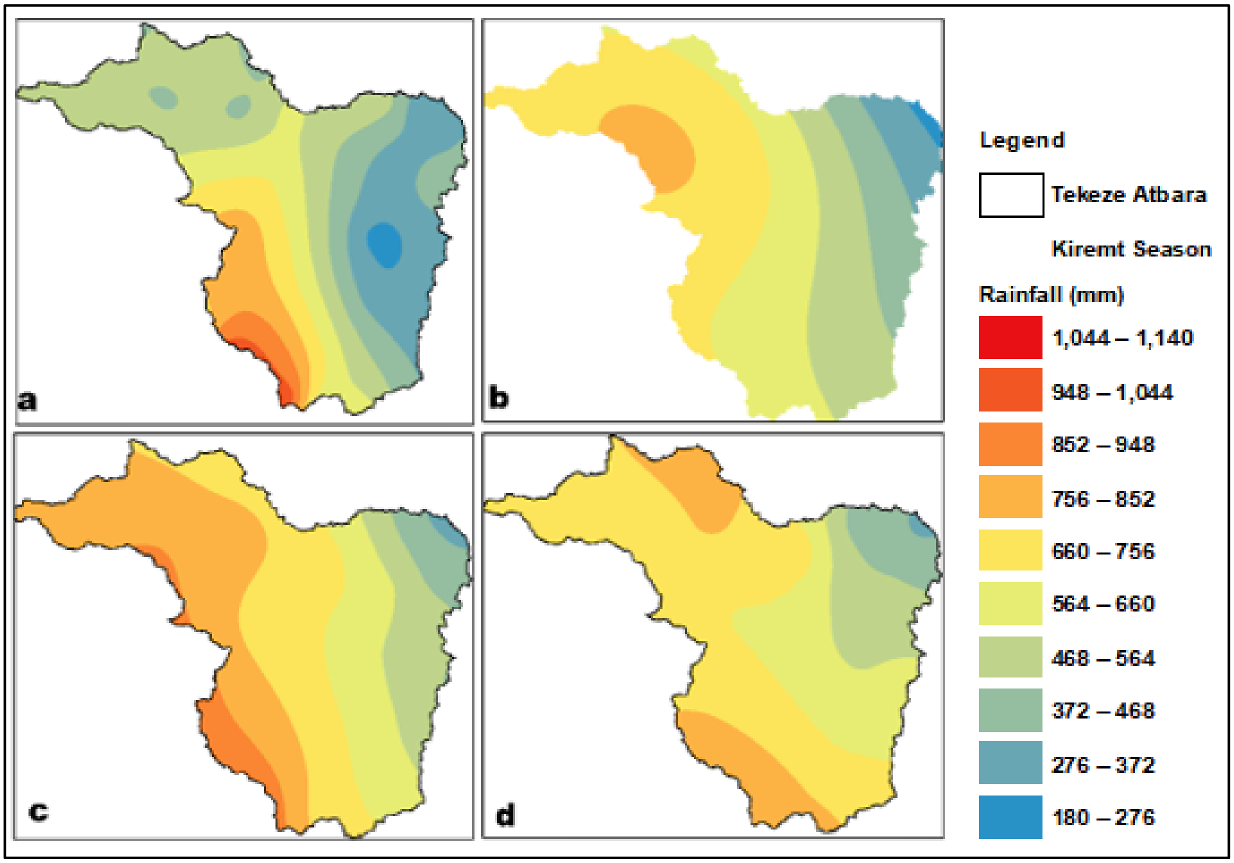


Figure 8. Comparison of the spatial pattern of mean seasonal rainfall for the kiremt season (June to September); a) Observed, b) PERSIANN_CDR, c) CHIRPS and d) TMPA 3B42 over the UTARB for the period 2007-2017.

In the bega season, CHIRPS reproduced well the spatial pattern of the observed rainfall in all parts of the basin (Figure 9). PERSIANN_CDR showed a good pattern in the northern and southern parts of the basin, whereas it was overestimated in the central parts of the basin. TMPA 3B42 performed poorly in most parts, which was caused by a significant overestimation of the observed rainfall.

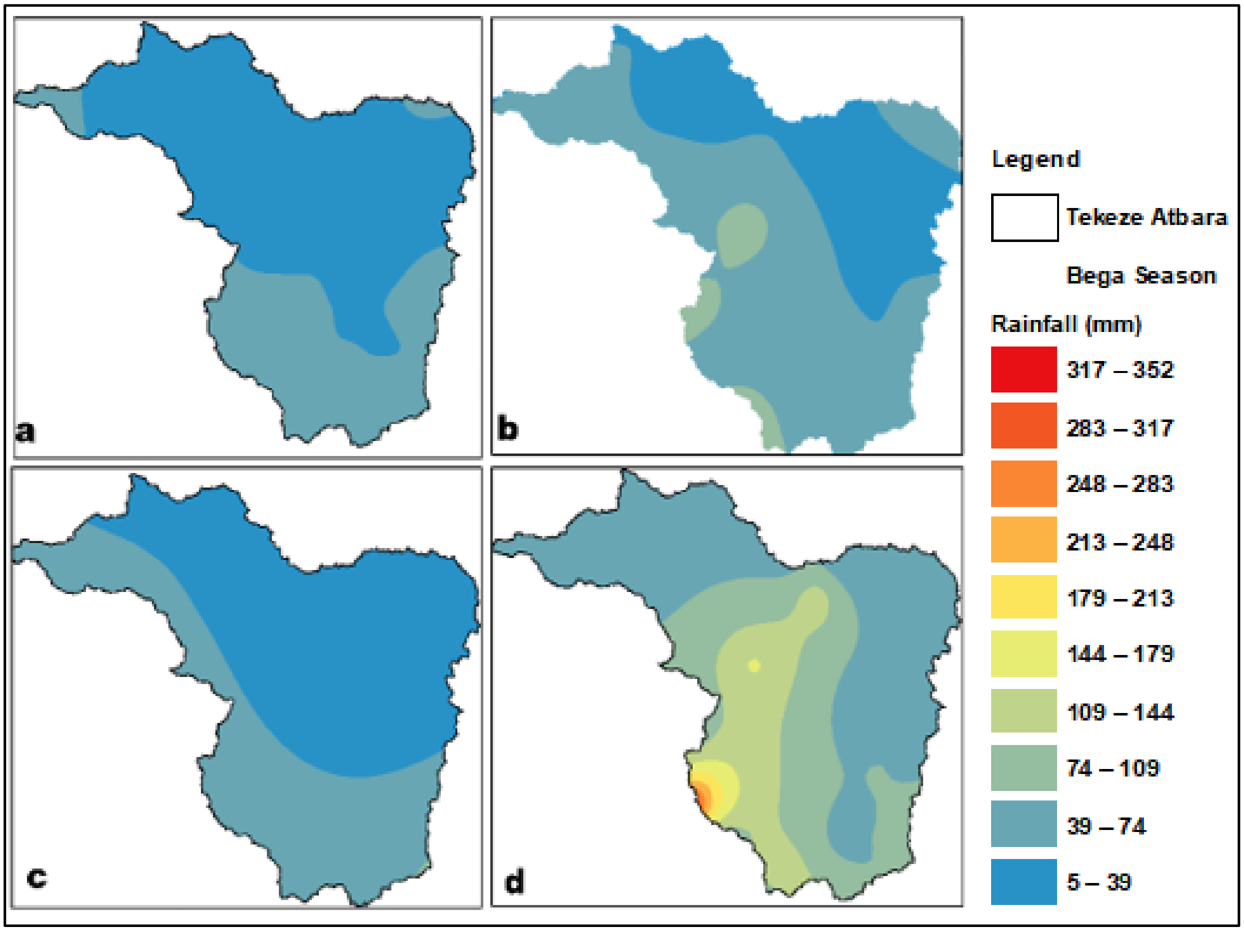


Figure 9. Comparison of the spatial pattern of mean season rainfall for the Bega season (October to January), a) Observed, b) PERSIANN_CDR, c) CHIRPS and d) TMPA 3B42 over the UTARB for the period 2007-2017.

**Rainfall Detection**

**Rainfall Event Detection**

All the three SRPs detected well the observed rainfall events, with the POD values > 0.7 (Figure 10). The TMPA 3B42 had the highest POD (0.81), while CHIRPS had the lowest POD (0.70). The highest potential of rainfall detection in TMPA 3B42 may associate with the retrieval algorithm of the product. Besides, all the SRPs had very high CSI values ranging from 0.64 to 0.73, indicating more than 64% of the observed rainfall events were correctly detected by the SRPs. However, the SRPs estimation missed some observed rainfall events. PERSIANN_CDR had the lowest FAR value (0.10), while TMPA 3B42 had the highest FAR value (0.15) which indicates that about 15% of estimated rainfall, but there was no observed rainfall event.

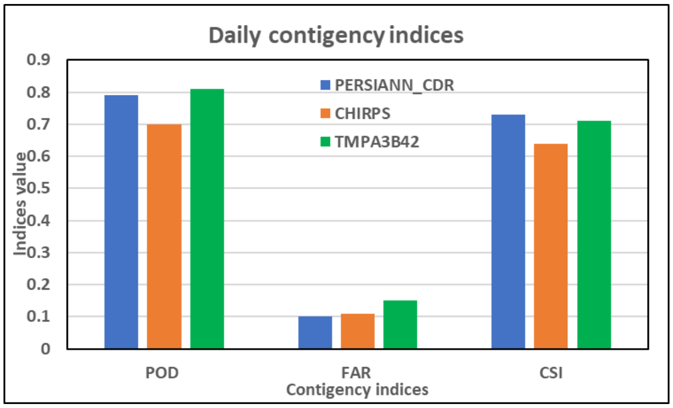


Figure 10. Summary of daily contingency indices (rainfall detection) comparison of satellite rainfall products with observed rainfall over the UTARB for the period 2007-2017.

As shown in Figure 11, the three products had the best detecting skill in the kiremt season with the highest POD value (≥ 90%) and CSI value (≥ 88%), and the lowest FAR value (≤ 3%). However, all the SRPs had the worst performance in detecting the rainfall in the bega season with the lowest POD (≤ 58%) and CSI (≤ 36%), and the highest FAR values (≥ 41%). In the kiremt season, more than 90% of the observed rainfall events were correctly detected by SRPs, with the highest value of 94% in PERSIANN_CDR and TMPA 3B42 products. Both products correctly detected 94% of the observed rainfall events. In the bega season, less than 58% of the observed rainfall events were correctly detected by SRPs. The CHIRPS correctly detected only 45% of the observed bega season rainfall. All rainfall products had nearly equivalent skills in detecting the kiremt season with FAR values less than ≤3%. However, the SRPs falsely detected the observed rainfall events by more than 41% in the bega season, with the highest value of 51% in the TMPA 3B42 product. The result from CSI showed that during the kiremt season, the PRSIANN_CDR and TMPA 3B42 products exhibited an equivalent CSI value (92%) of the rainfall events were correctly detected followed by CHIRPS (88%). In the bega season, the PRSIANN_CDR exhibited the highest CSI value (39%) followed by TMPA 3B42 (36%) and CHIRPS (33%).

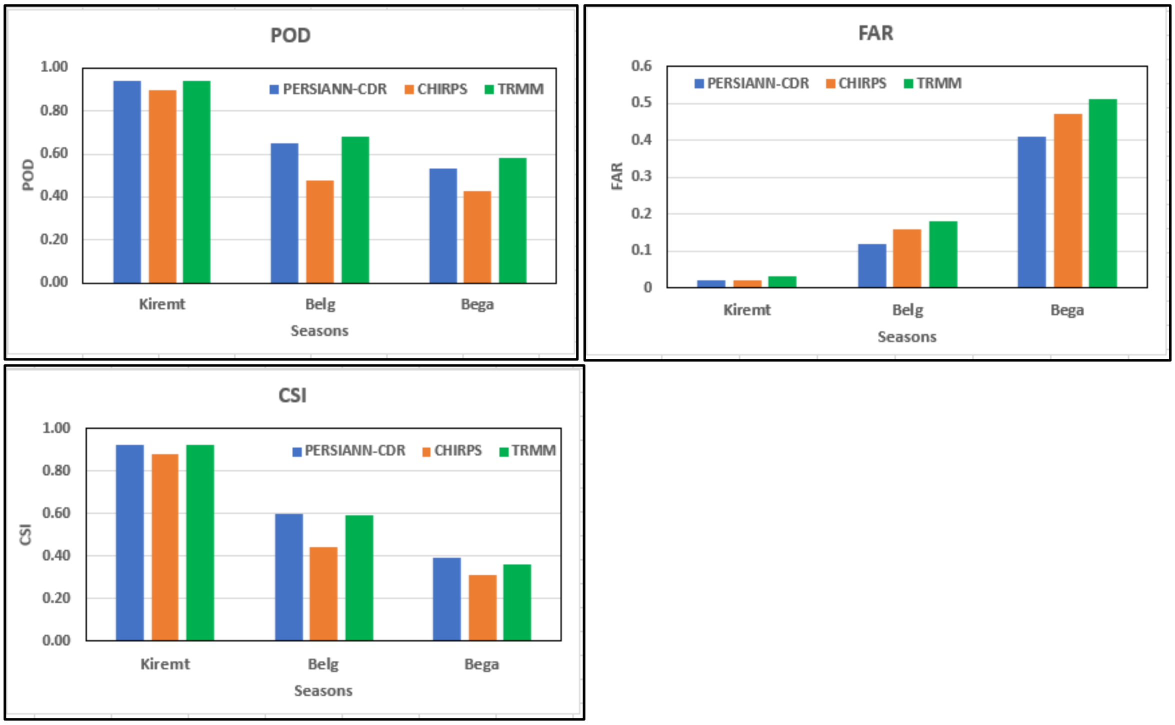


Figure 11. Comparisons of categorical indices (POD, FAR, & CSI) for kiremt, belg, and bega seasons over UTARB from a period 2007-2017.

The comparison between observed and SRPs frequencies detection for different rainfall classes is shown in Figure 12. All the three SRPs slightly underestimated the number of observed rainfall events less than 5 mm. However, the TMPA 3B42 product slightly overestimated the observed rainfall events between 5 mm and 10 mm, while PERSIANN_CDR and CHIRPS products slightly underestimated the observed rainfall events in the same range. All the SRPs overestimated the number of observed rainfall events between 10 mm and 50 mm (Figure 12), with the highest overestimation in the CHIRPS product. Both PERSIANN_CDR and TMPA 3B42 scored equal frequencies in rainfall events from 15-25 mm (heavy rain) and 25-50 mm (very heavy rainfall). In general, the PERSIANN_CDR had relatively a closer number of frequencies with observed rainfall in most classes.

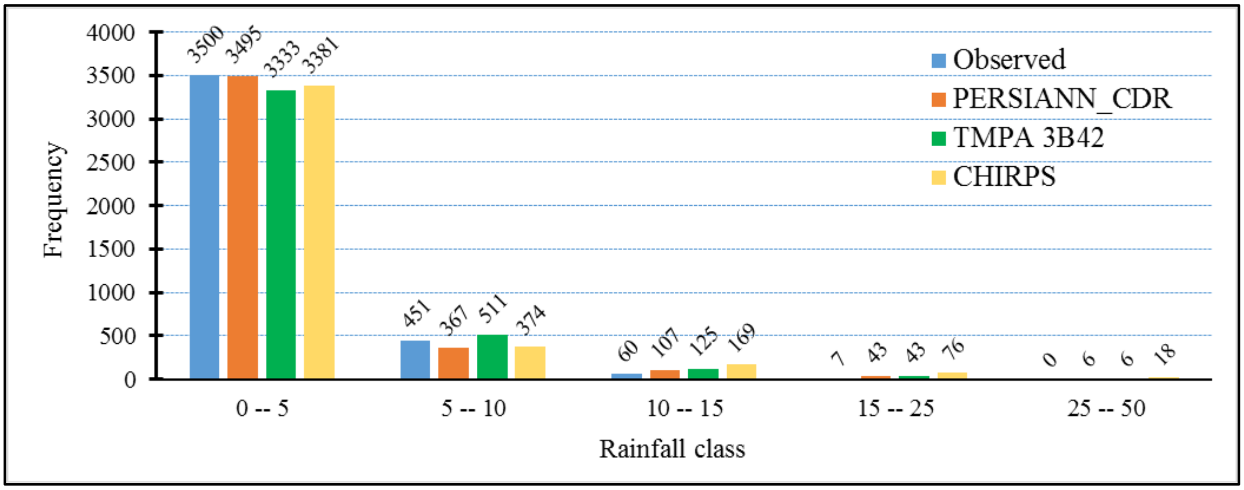


Figure 12. Comparisons of rainfall events at different classes between observed and SRPs.

**Rainfall Volume Detection**

Table 7 presents the missed and false rainfall volume detection potential of the three SRPs for the daily and seasonal time scale. The estimated missed rainfall volume (MRV) in the three SRPs were varied insignificantly for the daily and seasonal time scale, while the estimated false rainfall volume (FRV) was varied significantly in all time scale except kiremt season. CHIRPS had slightly lower MRV (1.1%) in daily rainfall (Table 7). On the contrary, the FRV value in the daily rainfall was low in PRSIANN_CDR and TMPA 3B42 products (3.3%).

Table 7. Comparisons of rainfall volume detection from daily and seasonal time scales.

| Satellite Rainfall | MRV (%) | | | | FRV (%) | | | |
|---|---|---|---|---|---|---|---|---|
| Products | Annual | Kiremt | Belg | Bega | Annual | Kiremt | Belg | Bega |
| PERSIANN_CDR | 1.2 | 0.38 | 3.6 | 4.2 | 3.3 | 0.52* | 6.4 | 28.4 |
| CHIRPS | 1.1 | 0.38 | 3.8 | 5.3 | 7.8 | 0.57 | 5.9 | 29.3 |
| TMPA3B42 | 1.3 | 0.34 | 3.6 | 4.4 | 3.3 | 0.67 | 10.8 | 50.2 |

Note: MRV= miss rainfall volume, FRV= false rainfall volume.

All SRPs had a lower MRV (0.34 to 0.38%) in the kiremt season. During belg season, PRSIANN_CDR and TMPA3B42 had equivalent MRV values (3.6%), while CHIRPS (3.8%) had slightly higher missed rainfall volume. During the bega season, the PRSIANN_CDR product had the lowest MRV value (4.2%) while CHIRPS had the highest MRV (5.3%). TMPA 3B42 had a higher false rainfall volume (FRV=50.2%) than CHIRPS (29.3%) and PRSIANN_CDR (28.4%) during the bega season. In the belg season, TMPA 3B42 had a higher FRV value (10.8%) than PRSIANN_CDR (6.4%) and CHIRPS (5.9%). Also, TMPA 3B42 had slightly a higher FRV value (0.67%) than CHIRPS (0.57%) and PRSIANN_CDR (0.52%) during the kiremt season.

## DISCUSSIONS

The PERSIANN_CDR had a lower PBIAS (5.3%), indicating a slight overestimation of the observed rainfall. However, the CHIRPS and TMPA 3B42 products significantly overestimated the observed rainfall by 23% and 18.8%, respectively. Fine temporal resolution, significant rainfall variability in topographically complicated locations, and the scale disparity between SRPs and observed rainfalls all contributed to these satellite-derived products' poor performance on a daily time scale (Rahmawati and Lubczynski, 2017). The PERSIANN_CDR had a strong association with the observed monthly rainfalls. And the association significantly improved in monthly bases compared to the daily timescale. The same result in Conti et al. (2014) found that the overall performance of SRPs improves from one to five days and then stabilizes as temporal aggregation grows. Increasing the temporal scale (daily to monthly) resulted in better agreements between the interpolated rain gauge data and other precipitation products (Zambrano-Bigiarini et al., 2017).
Results from PBIAS showed that the PERSIANN_CDR and CHIRPS performed a lower overestimation of the observed rainfall during the belg season, with a value of 3.1% and 2.0% respectively. The two products estimated a higher overestimation during the bega season, while PERSIANN_CDR estimated a lower overestimation during kiremt season which indicates that the contribution of injecting gauge observation into the model to improve the SRPs. The inability of the TIR sensor to distinguish cirrus clouds from rain clouds accounts for the overestimation of CHIRPS during the kiremt season (Thiemig et al., 2012; Young et al., 2014; Dinku et al., 2014; Toté et al., 2015; Mewcha et al., 2021). Furthermore, during the kiremt season, the CHIRPS exaggerated in-situ observation (28.6 percent). This backs up the views of Zambrano-Bigiarini et al. (2017) and Fenta et al. (2018), who stated that satellite-derived products may perform differently in different regions due to regional and/or local characteristics, requiring validation and bias adjustment before being used in hydrological studies.

The CHIRPS product had a lower PBIAS (17.9%) than PERSIANN_CDR (27.4%) and TMPA 3B42 (80.8%) in the bega season. This result is similar to Zolina et al., 2004; Sun et al., 2006; Lopez, 2007; Funk et al., 2015; Skok et al., 2015). The use of TMPA 3B42 for establishing the regression equations linking infrared-based cold-cloud duration values to mean rainfall resulted in too few dry days in CHIRPS, which was attributed to the use of TMPA 3B42 for establishing the regression equations linking infrared-based cold-cloud duration values to mean rainfall (Funk et al., 2015; Beck et al., 2017). The presence of spurious drizzle produced by flaws in the modeling and/or parameterization of the physical mechanisms regulating rainfall formation caused the reanalyses to regularly underestimate the number of dry days around the world (Zolina et al., 2004; Sun et al., 2006; Lopez, 2007; Skok et al., 2015). The higher PBIAS during the bega season in PERSIANN_CDR can be related to higher evaporation of the rainfall before it reaches the land surface. Hence, evaporation from surface rain gauges during the dry season could lead to the overestimation of rainfall from rain gauges by satellite rainfall products.

In general, the three SRPs represented well the observed rainfall in all seasons. The PERSIANN_CDR rainfall estimate had a good correlation with observed rainfall in all seasons. However, TMPA 3B42 rainfall estimates had a higher percent of detection (POD) on the observed rainfall values than the two products in all seasons. The technique of translating infrared CCD measurements into precipitation estimates using the 0.25° grid cell TMPA datasets, which could result in the formation of too much light rain, could be linked to CHIRPS' overestimation of wet days (Funk et al., 2015). These findings show that the quality of accessible rainfall products for daily to monthly time intervals varies greatly. The current study's spatial-temporal analysis of the products identified some of the sources of errors, such as the effect of various sensors, topography, and the retrieval algorithm (Beighley et al., 2011; Qin et al., 2014).

## CONCLUSIONS

This study comprehensively evaluated the applicability and reliability of SRPs (PERSIANN_CDR, CHIRPS, and TMPA 3B42) over the Upper Tekeze-Atbara River Basin for the period from 2007 to 2017. The CHIRPS had higher PBIAS in daily timescale followed by TMPA 3B42, while PERSIANN_CDR had very low positive PBIAS.

The comparative analysis showed that the PERSIANN_CDR outperform in continuous statistical error metrics (CC, RMSE, and PBIAS) for daily, monthly and seasonal time scales followed by CHIRPS and TMPA 3B42. Moreover, the PERSIANN_CDR showed very good skill in detecting rainfall events (POD, FAR, and CSI) and volume (MRV & FRV) from daily and seasonal scales. Overall, the results of this validation study suggest that the PERSIANN_CDR product has the potential to be used for a variety of operational applications, such as studying Spatio-temporal rainfall patterns and variability over the complicated topography of Ethiopia's Upper Tekeze-Atbara River Basin.

This study will be a useful reference for future applications of satellite rainfall estimates as inputs to hydrological models for the basin, especially in rain gauge sparse and ungauged basins with rugged terrains. We recommended that to get a full insight on the accuracy of satellite rainfall estimates, further studies on hydrological evaluation through streamflow simulation from different models (e.g., SWAT, HBV-light, HEC-HMS). And evaluating the effects of different bias correction methods on model simulations should be applied over the basin.

**Acknowledgments**
The authors acknowledge the National Meteorological Service Agency of Ethiopia (NMSA) for providing rainfall data (http://www.ethiomet.gov.et). We also acknowledge the University of Gondar for the support of fund and office services (http://www.uog.edu.et).

**Data Availability**
The rainfall data used to support the findings of this study are available from the corresponding author upon request.

**Declaration of Competing Interest**

The authors declare that they have no known competing financial interests or personal relationships that could have appeared to influence the work reported in this paper.

**References**

Alemu M.M., and Bawoke G.T., 2019. Analysis of spatial variability and temporal trends of rainfall in Amhara region, Ethiopia. J. Water Clim. Chang.

Ashouri H., Hsu K.L., Sorooshian S., Braithwaite D.K., Knapp K.R., Cecil L.D., Nelson B.R., and Prat O.P., 2015. PERSIANN_CDR: Daily precipitation climate data record from multi-satellite observations for hydrological and climate studies. Bulletin of the American Meteorological Society, 96(1), 69-83. doi:10.1175/BAMS-D-13–00068.1.

Awulachew S.B., Denekew A., Loulseged Y.M., Loiskandi W., Ayana M., and Alamirew T., 2007. IWMI Water Resources and Irrigation Development in Ethiopia; Working Paper 123; IWMI: Colombo, Sri Lanka.

Ayalew D., Tesfaye K., Girma M., Birru Y., and Wondimu B., 2012. Variability of rainfall and its current trend in Amhara region, Ethiopia African Journal of Agricultural Research 7(10), 1475–1486. https://doi.org/10.5897/ajar11.698.

Ayehu G.T., Tadesse T., Gessesse B., and Dinku T., 2018. Validation of new satellite rainfall products over the Upper Blue Nile Basin, Ethiopia. Atmos. Meas. Tech.11, 1921–1936.

Behrangi A., Khakbaz B., Jaw T.C., AghaKouchak A., Hsu K., and Sorooshian, S., 2011. Hydrologic evaluation of satellite precipitation products over a mid-size basin, Journal of Hydrology, 397, 225–237.

Beighley R.E., Ray R.L., He Y., Lee H., Schaller L., Andreadis K.M., Durand M., Alsdorf D.E., and Shum C.K., 2011. Comparing satellite-derived precipitation datasets using the Hillslope River Routing (HRR) model in the Congo River Basin. Hydrol. Process. 25, 3216–3229.

Belete K., 2007. Sedimentation and sediment handling at dams in Tekeze River Basin, Ethiopia (Doctoral dissertation, Norwegian University of Science and Technology).

Bostan, P.A., Heuvelink, G.B. and Akyurek, S.Z., 2012. Comparison of regression and kriging techniques for mapping the average annual precipitation of Turkey. International Journal of Applied Earth Observation and Geoinformation, 19, pp.115-126.

CHIRPS Website; http://chg.geog.ucsb.edu/data/chirps/ (last accessed March 9, 2021). Or the KNMI Climate Explorer Web page; http://climexp.knmi.nl/selectdailyfield.cgi/ (last accessed March 13, 2021).

Conway, D., 2000. The climate and hydrology of the upper Blue Nile River. The Geographical Journal 166, 49–62.

Diem J.E., Hartter J., Ryan S.J., and Palace M.W., 2014. Validation of satellite-based rainfall products for western Uganda. Journal of Hydrometeorology, 15(5), 2030– 2038.

Dinku T., Ceccato P., Grover-Kopec E., Lemma M., Connor S.J., and Ropelewski C.F., 2007. Validation of satellite rainfall products over East Africa's complex topography. Int. J. Remote Sens. 28, 1503–1526.

Dinku T., Hailemariam K., Maidment R., Tarnavsky E., and Connor S., 2014. Combined use of satellite estimates and rain gauge observations to generate high-quality historical rainfall time series over Ethiopia. Int. J. Climatol. 34, 2489–2504.

Dinku T., Funk C., Peterson P., Maidment R., Tadesse T., Gadain H., and Ceccato P., 2018. Validation of the CHIRPS satellite rainfall estimates over eastern Africa. Q. J. R. Meteorol. Soc. 114, 292–312.

Diro, G.T., Grimes, D.I.F., Black, E., O'Neill, A. and Pardo-Iguzquiza, E., 2009. Evaluation of reanalysis rainfall estimates over Ethiopia. International Journal of Climatology: A Journal of the Royal Meteorological Society, 29(1), pp.67-78.

Fenta A. A., Yasuda H., Shimizu K., Ibaraki Y., Haregeweyn N., Kawai T., Belay A.S., Sultan D., and Ebabu K., 2018. Evaluation of satellite rainfall estimates over the Lake Tana basin at the source region of the Blue Nile River. Atmos. Res. 212, 43–53.

Funk C., Peterson P., Landsfeld M., Pedreros D., Verdin J., Shukla S., Husak G., Rowland J., Harrison L., and Hoell A., 2015. The climate hazards infrared precipitation with stations—a new environmental record for monitoring extremes. Scientific data, 2, 150066.

Gao Y.C., and Liu M.F., 2013. Evaluation of high-resolution satellite precipitation products using rain gauge observations over the Tibetan Plateau. Hydrol. Earth Syst. Sci., 17, 837–849.

Gebrechorkos S.H., Hülsmann S., and Bernhofer C., 2017. Evaluation of multiple climate data sources for managing environmental resources in East Africa. Hydrology and Earth System Sciences, 22(8), pp.4547-4564.

Haile A.T., Rientjes T., Gieske A., and Gebremichael M., 2009. Rainfall variability over mountainous and adjacent lake areas: The case of Lake Tana basin at the source of the Blue Nile River. J. Appl. Meteorol. Climatol., 48, 1696–1717.

Hirpa F.A., and Gebremichael M., Hopson T., 2010. Evaluation of high-resolution satellite precipitation products over very complex terrain in Ethiopia, Journal of Applied Meteorology and Climatology, 49, 1044–1051.

Hobouchian M.P., Salio P., García Skabar Y., Vila D., and Garreaud R., 2017. Assessment of satellite precipitation estimates over the slopes of the subtropical Andes. Atmos. Res., 190, 43–54.

Huffman G., Bolvin D., Nelkin E., Wolff D., Adler R., Gu G., Hong Y., Bowman K., and Stocker E., 2007. The TRMM Multi-satellite Precipitation Analysis (TMPA): Quasi- Global, Multiyear, Combined-Sensor Precipitation Estimates at Fine Scales, J. Hydrometeorol., 8, 38–55.

Huffman G.J., Adler R.F., Bolvin D.T., and Nelkin, E.J., 2010. The TRMM multi-satellite precipitation analysis (TMPA), in Satellite rainfall applications for surface hydrology, edited by: Gebremichael, M. and Hossain, F., Springer, Dordrecht, 3–22.

Husak G.J., Michaelsen J., and Funk C., 2007. Use of the gamma distribution to represent monthly rainfall in Africa for drought monitoring applications. International Journal of Climatology: A Journal of the Royal Meteorological Society, 27(7), pp.935-944.

Iqbal M.F., and Athar H., 2018. Validation of satellite-based precipitation over diverse topography of Pakistan. Atmos. Res. 201, 247–260.

Jiang S., Ren L., Hong Y., Yong B., Yang X., Yuan F., and Ma M., 2012. Comprehensive Evaluation of Multi-Satellite Precipitation Products with a Dense Rain Gauge Network and Optimally Merging Their Simulated Hydrological Flows Using the Bayesian Model Averaging Method. Journal of Hydrology 452: 213–225. Doi: 10.1016/j.jhydrol.2012.05.055.

Katsanos D., Retalis A., and Michaelides S., 2016. Validation of a high-resolution precipitation database (CHIRPS) over Cyprus for 30 years. Atmos. Res. 169, 459–464.

Khan S.I., Yang H., Wang J., Yilmaz K.K., Gourley J.J., Adler R.F., Brakenridge G.R., Policell F., Habib S., and Irwin D., 2011. Satellite remote sensing and hydrologic modeling for flood inundation mapping in Lake Victoria basin: Implications for hydrologic prediction in ungauged basins. IEEE Trans. Geosci. Remote Sens., 49, 85–95.

Lakew H.B., Moges S.A., and Asfaw D.H., 2017. Hydrological Evaluation of Satellite and Reanalysis Precipitation Products in the Upper Blue Nile Basin: A Case Study of Gilgel Abbay. Hydrology. 4, 39.

Lekula M., Lubczynski M.W., Shemang E.M., and Verhoef W., 2018. Validation of satellite-based rainfall in Kalahari. Phys. Chem. Earth.105, 84–97.

Li Z., Yang D.W., and Hong Y., 2013. Multi-scale evaluation of high-resolution multi-sensor blended global precipitation products over the Yangtze River. J. Hydrol. 2013, 500, 157–169.

Lopez P., 2007. Cloud and precipitation parameterizations in modeling and variational data assimilation: a review, Journal of the Atmospheric Sciences, 64, 3766–3784.

National Meteorology Service Agency, 1996. Climatic and Agroclimatic Resources of Ethiopia; NMSA: Addis Ababa, Ethiopia.

Nyssen J., Vandenreyken H., Poesen J., Moeyersons J., Deckers J., Haile M., Salles, G., and Govers G., 2005. “Rainfall Erosivity and Variability in the Northern Ethiopian Highlands.” Journal of Hydrology 311: 172–187. Doi: 10.1016/j.jhydrol.2004.12.016.

Park N.W., Kyriakidis P.C., and Hong S., 2017. Geostatistical integration of coarse-resolution satellite precipitation products and rain gauge data to map precipitation at fine spatial resolutions. Remote Sensing, 9(3), p.255.

PERSIANN Website; http://chrsdata.eng.uci.edu (last accessed on March 9, 2021)

Qin Y., Chen Z., Shen Y., Zhang S., and Shi R., 2014. Evaluation of satellite rainfall estimates over the Chinese mainland. Remote Sens. 6, 11649–11672.

Rahmawati N., and Lubczynski M.W., 2017. Validation of satellite daily rainfall estimates in the complex terrain of Bali Island, Indonesia. Theor. Appl. Climatol. 1–20. https://doi.org/10.1007/s00704-017-2290-7.

Rientjes T., Haile A.T., and Fenta A.A., 2012. Diurnal rainfall variability over the Upper Blue Nile Basin: A remote sensing-based approach. Int. J. Appl. Earth Obs. Geoinf. 21, 311–325.

Rivera J.A., Marianetti G., and Hinrichs S., 2018. Validation of CHIRPS precipitation dataset along the Central Andes of Argentina. Atmos. Res. 213, 437–449.

Sahlu D., Moges S.A., Nikolopoulos E.I., Anagnostou E.N., and Hailu D., 2017. Evaluation of High-Resolution Multi-satellite and Reanalysis Rainfall Products Over East Africa. Advances in Meteorology, 2017.

Santhi C., Arnold J.G., Williams J.R., Dugas W.A., Srinivasan R., and Hauck L.M., 2001. Validation of the SWAT Model on a Large River Basin with Point and Nonpoint Sources. Journal of the American Water Resources Association 37(5):1169-1188.

Segele Z., 2008, January. Wavelet-Based Monthly-to-Seasonal Rainfall Predictions for Ethiopia. In 20th Conference on Climate Variability and Change.

Seleshi Y., and Zanke U., 2004. Recent changes in rainfall and rainy days in Ethiopia. International Journal of Climatology: A Journal of the Royal Meteorological Society, 24 (8), pp.973-983.

Skok G., Žagar N., Honzak L., Žabkar R., Rakovec J., and Ceglar A., 2016. Precipitation Intercomparisons of a set of satellite and Raingauge-derived datasets, ERA-Interim reanalysis, and a single WRF regional climate simulation over Europe and the North Atlantic. Theoretical and applied climatology, 123(1-2), pp.217-232.

Stillman S., Ninneman J., Zeng, X., Franz, T., Scott, R., Shuttleworth, W., and Cummins, K., 2014. Summer Soil Moisture Spatiotemporal Variability in Southeastern Arizona, J. Hydrometeorol., 15, 1473–1485, https://doi.org/10.1175/JHM-D-13-0173.1.

Sun Y., Solomon S., Dai A., and Portmann R.W., 2006. How often does its rain? Journal of Climate, 19, 916–934.

Sutcliffe J.V., and Parks, Y.P., 1999. The hydrology of the Nile.

Tamene L., Park S.J., Dikau R., and Vlek P.L.G., 2006. Analysis of factors determining sediment yield variability in the highlands of northern Ethiopia. Geomorphology, 76 (1-2), pp.76-91.

Taylor K.E., 2001. Summarizing multiple aspects of model performance in a single diagram, J. Geophys. Res.-Atmos., 106, 7183–7192, https://doi.org/10.1029/2000jd900719.

Thiemig V., Rojas R., Zambrano-Bigiarini M., Levizzani V., and de Roo A., 2012. Validation of satellite-based precipitation products over sparsely gauged African river basins, Journal of Hydrometeorology, 13, 1760–1783.

TRMM webpage; https://disc.gsfc.nasa.gov (last accessed March 9, 2021).

Yong B., Ren L.L., Hong Y., Wang J.H., Gourley J.J., Jiang S.H., Chen X., and Wang W., 2010. Hydrologic evaluation of multi-satellite precipitation analysis standard precipitation products in basins beyond its inclined latitude band: A case study in Laohahe basin, China. Water Resour. Res., 46, W07542.

Young M., Williams C., Chiu J., Maidment R., and Chen, S., 2014. Investigation of Discrepancies in Satellite Rainfall Estimates Over Ethiopia, J. Hydrometeor.,15, 2347-2369, Doi: 10.1175/JHM-D-13-0111.1.

Zambrano-Bigiarini M., Nauditt A., Birkel C., Verbist K., and Ribbe L., 2017. Temporal and spatial evaluation of satellite-based rainfall estimates across the complex topographical and climatic gradients of Chile. Hydrol. Earth Syst. Sci. 21, 1295–1320.

Zhang, K., Kimball, J.S. and Running, S.W., 2016. A review of remote sensing-based actual evapotranspiration estimation. Wiley Interdisciplinary Reviews: Water, *3*(6), pp.834-853.

Zolina O., Kapala A., Simmer C., and Gulev S.K., 2004. Analysis of extreme precipitation over Europe from different reanalyses: a comparative assessment. Global and Planetary Change, 44(1-4), pp.129-161.